Charge Carrier Dynamics in Small-Molecule- and Polymer-based Donor-Acceptor Blends

Charge carrier dynamics in small-molecule- and polymer-based donor-acceptor blends

Keshab Paudel[1], Brian Johnson[1], Mattson Thieme[1], John E. Anthony[2], Oksana Ostroverkhova[1]
[1]Oregon State University, Corvallis, OR, United States.
[2]University of Kentucky, Lexington, KY, United States.

ABSTRACT

We present a comparative study of optical absorption, photoluminescence (PL), and photoconductivity in bulk heterojunctions comprising a high performance functionalized anthradithiophene (ADT) derivative or the benchmark polymer P3HT as donor and functionalized pentacene (Pn) derivative or PCBM as acceptor. Of all D/A blends studied, the ADT/PCBM blend exhibited the highest charge photogeneration efficiencies under 532 nm excitation, leading to the highest amplitudes of time-resolved and continuous wave (cw) photocurrents. At nanosecond time scales after photoexcitation, both ADT-TES-F-based blends and the P3HT/Pn-TIPS-F8 blend exhibited photocurrents which were higher by a factor of 2-10, depending on the blend, than that in the P3HT/PCBM blend. However, cw photocurrents showed a different trend, with the ADT-TES-F/PCBM blend exhibiting only a factor of ~2.5 higher photoresponse than that in the P3HT/PCBM blends, and the ADT-TES-F- and P3HT- based blends with Pn-TIPS-F8 showing a factor of ~1.5-2.5 lower photoresponse than that in the P3HT/PCBM blend, due to other contributions, such as that of charge trap-limited transport, to cw photoresponse.

INTRODUCTION

Organic semiconductors have attracted attention due to their potential applications in low-cost (opto)electronic devices. For applications that rely on charge carrier photogeneration, such as photovoltaic devices, donor-acceptor (D/A) bulk heterojunctions (BHJs) are of particular interest, and optimization of relative energies, molecular packing, and other parameters to achieve the highest possible photocurrents has been a subject of considerable research.[1] So far, the best performing BHJs utilize a polymer donor and a fullerene acceptor. In these systems, power conversion efficiencies (PCEs) of up to 10-12% have been reported.[1] Significant progress has also been made in the development of small-molecule (SM) BHJs, with the PCEs of ~9% for solution deposited BHJs and up to 10.1% for tandem cells.[2] However, both polymer-based and SM BHJs with non-fullerene acceptors significantly underperform; for example, the best non-fullerene SMBHJs currently exhibit PCEs of only ~3.1%.[3] Since fullerene derivatives have a number of drawbacks,[4] it is important to develop alternative acceptor molecules and to understand how the properties of resulting D/A BHJs depend on the properties of the D and A molecules.

In this paper, we present comparative studies of the optical, photoluminescent (PL), and photoconductive properties of several types of D/A BHJs, in particular (i) SM donor/SM non-fullerene acceptor, (ii) SM donor/SM fullerene acceptor, (iii) polymer/SM non-fullerene acceptor, and (iv) polymer/SM fullerene systems. Donor-only films were also prepared, and their properties were compared to those of the D/A blends.

EXPERIMENTAL

Materials

For this study, we chose a functionalized fluorinated anthradithiophene (ADT) derivative with triethylsilylethynyl (TES) side groups (ADT-TES-F) and regio-regular P3HT as the donors and fluorinated pentacene (Pn) functionalized with triisopropylsilylethynyl (TIPS) groups (Pn-TIPS-F8) and $PC_{61}BM$ as acceptors (Fig.1(a)). The motivation behind this choice was as follows. The ADT-TES-F derivative exhibits hole mobilities of over 1.5 cm^2/Vs (up to 6 cm^2/(Vs)) in spin-cast thin-film (single crystal) transistors,[5,6] in which efficient charge transport is enabled by molecular packing into a 2D "brick-work" π-stacked structure with strong π–π overlap. Additionally, ADT-TES-F films exhibit fast charge carrier photogeneration and high photoconductive gains.[7] The P3HT is a benchmark polymer donor, which has been extensively utilized in BHJ solar cells. Fullerene acceptors, such as PCBM, have been previously shown to improve charge photogeneration efficiency in both ADT-TES-F-based and P3HT-based D/A blends.[8] Addition of the Pn-TIPS-F8 acceptor to the ADT-TES-F donor has been shown to result in the formation of an emissive charge transfer state (exciplex), which was detrimental for charge photogeneration.[9] Photoinduced interactions between P3HT and Pn-TIPS-F8 and their effect on photoconductivity are not known; also not known is how charge carrier dynamics in P3HT-based D/A blends compare to those in ADT-TES-F-based D/A blends utilizing same acceptors, which is investigated here.

Sample preparation

30 mM solutions of each compound were prepared in chlorobenzene. Then, D/A blends ADT-TES-F/Pn-TIPS-F8 and ADT-TES-F/PCBM were prepared at 1:1 and 9:1 wt./wt. proportions, and various proportions were prepared of P3HT/Pn-TIPS-F8 and P3HT/PCBM blends. The choice of the relative D and A concentrations in the ADT-TES-F/PCBM blend was due to the highest photocurrents being achieved in ADT-TES-F/PCBM blends with PCBM concentrations in the 7-10 wt% range.[10] The D/A film samples were prepared by spin-casting 10 µL of the solution at 3000 rpm for 30 seconds on glass substrates with 10 pairs of Cr/Au (5 nm/50 nm thick) interdigitated gold electrodes with a 25 µm gap. Just before spin-casting, each substrate was treated with pentafluorobenzenethiol (PFBT), which was found to form a self-assembled monolayer on the substrate and facilitate crystallization in fluorinated SMs such as
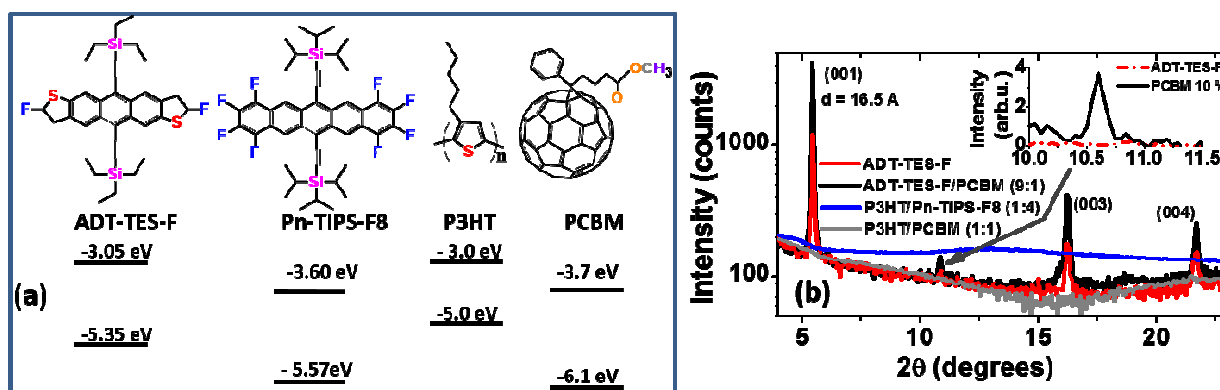
Figure 1. (a) Molecular structures and HOMO and LUMO energies of the materials used in our studies. (b) XRD data obtained from solution-deposited films. Inset shows a magnified view of the feature due to crystallization of PCBM in the ADT-TES-F/PCBM blend.

ADT-TES-F.[9] No annealing procedures were applied to any of the samples. Such film preparation method resulted in polycrystalline ADT-TES-F films and blends of ADT-TES-F with PCBM or Pn-TIPS-F8, as confirmed by the x-ray diffraction (XRD) (Fig. 1(b)).[10] In these films, ADT-TES-F crystallites had a predominant (00l) orientation (l =1, 3,4), in agreement with previous studies.[6] The ADT-TES-F/PCBM (9:1) blends exhibited crystalline domains of PCBM (inset of Fig. 1(b)) and enhanced ADT-TES-F crystallinity (Fig. 1(b)). In contrast, the addition of Pn-TIPS-F8 to ADT-TES-F reduced the crystalline order of ADT-TES-F, as discussed in our previous publication.[10] Films with P3HT did not show any significant crystalline order, which is expected from P3HT-based films which have not undergone a high-temperature annealing process.[11]

Measurement procedures

Optical absorption was taken in air at room temperature using an Ocean Optics USB2000-FLG spectrometer and LS-1 tungsten halogen lamp. PL spectra were obtained under 532 nm excitation (frequency doubled Nd : YVO$_4$ laser from Coherent, Inc.) and collected through a 537nm long pass filter (Chroma Tech.) by the USB2000-FLG spectrometer.

Currents in the dark and under a 100 µW continuous wave (cw) illumination with a 532 nm laser were measured using a Keithley 237 source-measure unit. Photocurrents were then calculated by subtracting dark currents from the corresponding currents under illumination. For transient photocurrent measurements, the Keithley 237 source-measure unit provided bias voltage to the sample, and signals were acquired with an Agilent DSO6032A 300MHz oscilloscope under 532 nm pulsed excitation (470 ps,55 kHz, Q-switched frequency doubled Nd:YAG laser, Altechna STA-01-SH-4-MOPA) at a fluence of ~1.4 $\mu J/cm^2$. Time resolution was ~ 1.0 ns, limited by the laser pulse width and the DSO response time. [8, 9,12,13] All the measurements were carried out in air at room temperature.

RESULTS AND DISCUSSION

Optical absorption and photoluminescence properties

Optical absorption spectra of the pristine films are shown in Fig. 2(a). Absorption spectra of D/A blends were a superposition of the absorbance of the blend constituents, with no apparent charge transfer bands between D and A.[14] Figure 2(b-c) shows the PL spectra of pristine and D/A films. In both the ADT-TES-F- and P3HT-based D/A blends, donor emission was considerably reduced, as compared to that in pristine donor (ADT-TES-F or P3HT) films, consistent with charge transfer from the donor to the acceptor. In the case of the ADT-TES-F/Pn-TIPS-F8 blend, strong PL emission due to the ADT-TES-F/Pn-TIPS-F8 CT state (exciplex) was observed, with a peak at ~ 710 nm (1.75 eV) (Fig. 2(b)) which closely matched the energy difference between the LUMO of Pn-TIPS-F8 and HOMO of ADT-TES-F.[9,10,12] No emissive CT states were observed in any other D/A blend studied.

Transient and cw photocurrents

Figure 3(a) shows TPCs in pristine ADT-TES-F films and several D/A blends under a 470 ps 532 nm excitation at an applied electric field of 40 kV/cm. (The linear photocurrent density, appropriate for planar device geometry used in our experiments,[16] was obtained by dividing the photocurrent by the channel width.) Pristine ADT-TES-F films and ADT-TES-F-based D/A blends exhibited higher TPC amplitudes than any of the P3HT-based blend studied, which is most likely related to crystalline order of ADT-TES-F-based films.[10]
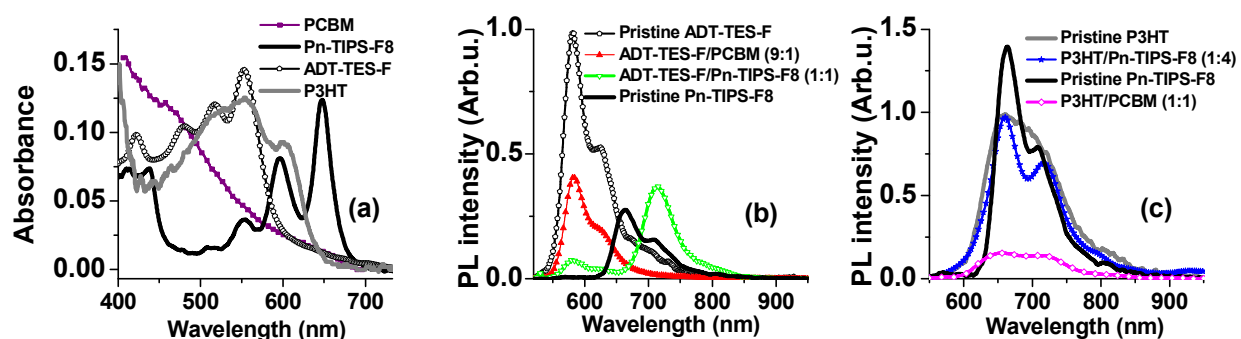
Figure 2. (a) Optical absorption spectra of pristine films. (b) and (c): PL spectra of pristine films and D/A blends used in our study.

Under the same experimental conditions, no TPCs were observed in pristine P3HT films or P3HT/Pn-TIPS-F8 films with Pn-TIPS-F8 concentrations lower than 80 wt%. In all samples in which the TPCs could be detected, the TPCs had a fast initial rise, limited by the time resolution of our measurement, and decay dynamics characterized by a fast component (<5 ns) and a slow component that in ADT-TES-F-based samples persisted up to at least μs time-scales.[7,13] The fast decay component has been previously attributed to charge trapping and various recombination processes such as bimolecular and trap-assisted recombination;[15] for example, a faster decay in ADT-TES-F/PCBM blends as compared to pristine ADT-TES-F films was determined to be due to enhanced bimolecular recombination in these blends.[10] The slower decay component has been previously attributed to dispersive transport.[8] In P3HT-based blends, the fast decay component was considerably more pronounced than in ADT-TES-F-based blends (Fig.3(b)). This indicates stronger charge carrier trapping and recombination in the disordered P3HT-based blends, as compared to crystalline ADT-TES-F-based blends, which considerably reduces the density of photogenerated mobile charge carriers within ~2 ns after photoexcitation. The ADT-TES-F/PCBM (9:1) blend exhibited the highest TPC amplitude of all blends studied, which was an order of magnitude higher than that in the P3HT/PCBM (1:1) blend (Fig.3(a)).

Figure 3(c) shows cw photocurrent obtained in various films under cw 532 nm excitation. In trend with the TPCs, the highest cw photocurrents were observed in the ADT-TES-F/PCBM films, followed by pristine ADT-TES-F films. These were followed by the P3HT/PCBM blend, which outperformed other films, in contrast to the trends in the ns-time-scale TPCs of Fig.3(a).[9,16,17] However, the cw photocurrents incorporate contributions to charge photogeneration at time scales longer than ns, trap-limited charge transport, and carrier injection from the electrodes, most of which do not contribute to the TPCs. For example, cw photocurrents in ADT-TES-F films and ADT-TES-F-based blends were found to scale with dark currents in these films,[9,16] which highlights the contributions of properties not related to charge photogeneration to cw photocurrents.

To gain further insight into the observed behavior, we summarized TPC amplitudes, integrated TPCs, cw photocurrents, and dark currents in various samples, relative to the corresponding values in the pristine ADT-TES-F film, in Fig. 4. In particular, the TPC amplitude is mostly determined by fast charge carrier generation efficiency and a sum of hole and electron mobilities.[10,15] The TPC integrated over 20 ns yields total extracted charge over this time period, thus incorporating carrier loss due to recombination and deep trapping. The dark currents depend on hole injection efficiency from the Au electrodes and on the hole mobility, and cw photocurrents incorporate all the above effects. For example, the enhancement in cw
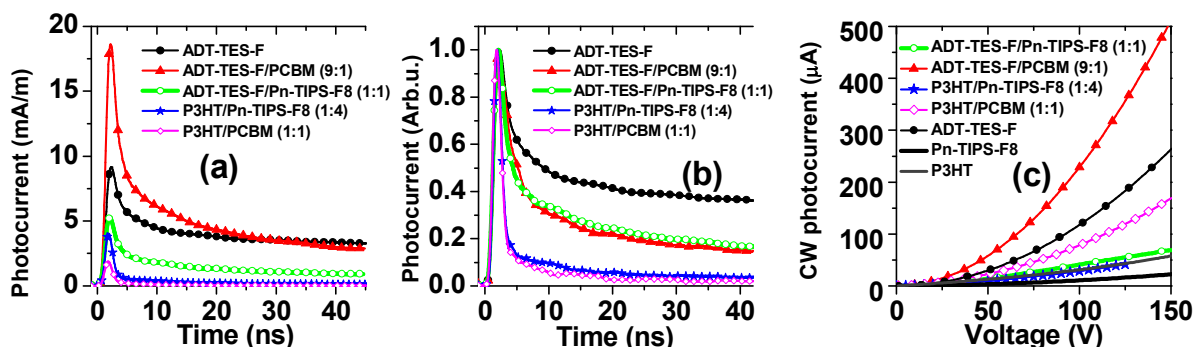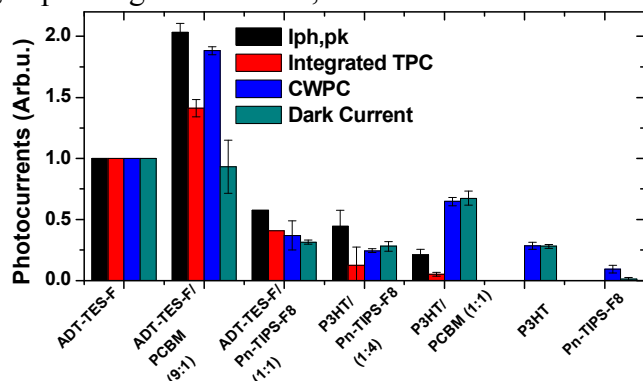
Figure 3. (a) Transient photocurrents measured in pristine films and in D/A blends under a pulsed 532 nm excitation at an applied electric field of 40 kV/cm. (b) Transient photocurrents from (a) normalized by the corresponding peak photocurrent values. (c) Cw photocurrents obtained in various films under 532 nm cw excitation.

photocurrent in the ADT-TES-F/PCBM blend as compared to that in the pristine ADT-TES-F film without increased dark currents suggests that such enhancement is due to the improved charge photogeneration efficiency, consistent with the high TPC amplitude in this blend. In contrast, the enhancement in cw photoresponse of the P3HT/PCBM blend as compared to that in ADT-TES-F/Pn-TIPS-F8 and P3HT/Pn-TIPS-F8 blends was accompanied by an increased dark current. Thus, it is not indicative of enhanced charge photogeneration and instead may suggest that morphology of the P3HT/PCBM blend is more conducive to efficient trap-limited charge transport[7,16] than that in the other two blends. The lower photo- and dark currents in ADT-TES-F/Pn-TIPS-F8 blends as compared to pristine ADT-TES-F films are due to reduced ADT-TES-F crystallinity in such blends which decreases charge generation efficiency and mobility.[10]

CONCLUSIONS

We explored optical, PL, and photoconductive properties of BHJs based on small-molecule ADT-TES-F and polymer P3HT donors and on fullerene and non-fullerene acceptors. Of all blends studied, the ADT-TES-F/PCBM blend, followed by pristine ADT-TES-F films, showed the highest charge photogeneration efficiencies under 532 nm excitation, resulting in higher amplitudes of time-resolved and cw photocurrents. Both ADT-TES-F-based and P3HT-based blends with the Pn-TIPS-F8 acceptor exhibited higher ns time-scale photocurrent by a factor of 2-10, depending on the blend, than that in the P3HT/PCBM blend. However, the cw photocurrent

Figure 4. Comparison between the transient photocurrent amplitudes ($I_{ph,pk}$), transient photocurrents integrated over a 20 ns time period, cw photocurrents (CWPC), and dark currents obtained in various films, all with respect to corresponding values in a pristine ADT-TES-F film for which at 40 kV/cm $I_{ph,pk}$ = 9.3 mA/m (Fig. 3(a)), CWPC = 120 μA (Fig. 3(c)), and dark current is 90 μA. Error bars reflect variations in the values relative to those in pristine ADT-TES-F films measured under the same conditions depending on the applied electric field.

showed different trends, with the ADT-TES-F/PCBM blend exhibiting only a factor of ~2.5 higher photoresponse than that in the P3HT/PCBM blends, and the ADT-TES-F and P3HT-based blends with Pn-TIPS-F8 showing a factor of ~1.5-2.5 lower photoresponse than that in the P3HT/PCBM blend. Comparisons between trends in the transient photocurrent, cw photocurrent, and dark current highlight contributions to cw photoresponse that are not related to fast charge carrier photogeneration and instead may be related to charge trap-limited transport. Further studies are necessary to utilize strong photoresponse such as that in crystalline ADT-TES-F/PCBM blends in devices such as photodetectors, phototransistors, and solar cells.

ACKNOWLEDGMENTS

REFERENCES

[1] M.C. Scharber and N.S. Sariciftci, Prog. Polym. Sci. **38**, 1929 (2013).

[2] Y. Liu, C.-C. Chen, Z. Hong, J. Gao, Y.M. Yang, H. Zhou, L. Dou, G. Li, and Y. Yang, Sci. Rep. **3**, 3356 (2013).

[3] A. Sharenko, D. Gehrig, F. Laquai, and T.-Q. Nguyen, Chem. Mater. **26**, 4109 (2014).

[4] J.E. Anthony, Chem. Mater. **23**, 583 (2011).

[5] D.J. Gundlach, J.E. Royer, S.K. Park, S. Subramanian, O.D. Jurchescu, B.H. Hamadani, a J. Moad, R.J. Kline, L.C. Teague, O. Kirillov, C. A. Richter, J.G. Kushmerick, L.J. Richter, S.R. Parkin, T.N. Jackson, and J.E. Anthony, Nat. Mater. **7**, 216 (2008).

[6] S.K. Park, D. A. Mourey, S. Subramanian, J.E. Anthony, and T.N. Jackson, Appl. Phys. Lett. **93**, 043301 (2008).

[7] A. Platt, J. Day, S. Subramanian, J. Anthony, and O. Ostroverkhova, J. Phys. Chem. C **113**, 14006 (2009).

[8] A. Platt, M. Kendrick, M. Loth, J. Anthony, and O. Ostroverkhova, Phys. Rev. B **84**, 235209 (2011).

[9] K. Paudel, B. Johnson, A. Neunzert, M. Thieme, B. Purushothaman, M.M. Payne, and J.E. Anthony, J. Phys. Chem. C **117**, 24752 (2013).

[10] K. Paudel, B. Johnson, M. Thieme, M.M. Haley, M.M. Payne, J.E. Anthony, and O. Ostroverkhova, Appl. Phys. Lett. **105**, 043301 (2014).

[11] Y. Kim, S. Cook, S.M. Tuladhar, S. a. Choulis, J. Nelson, J.R. Durrant, D.D.C. Bradley, M. Giles, I. McCulloch, C.-S. Ha, and M. Ree, Nat. Mater. **5**, 197 (2006).

[12] M.J. Kendrick, a. Neunzert, M.M. Payne, B. Purushothaman, B.D. Rose, J.E. Anthony, M.M. Haley, and O. Ostroverkhova, J. Phys. Chem. C **116**, 18108 (2012).

[13] J. Day, A.D. Platt, O. Ostroverkhova, S. Subramanian, J.E. Anthony, Appl. Phys. Lett. **94**, 013306 (2009).

[14] W.E.B. Shepherd, A.D. Platt, M.J. Kendrick, M. A. Loth, J.E. Anthony, and O. Ostroverkhova, J. Phys. Chem. Lett. **2**, 362 (2011).

[15] B. Johnson, M.J. Kendrick, and O. Ostroverkhova, J. Appl. Phys. **114**, 094508 (2013).

[16] J. Day, A. D. Platt, S. Subramanian, J.E. Anthony, and O. Ostroverkhova, J. Appl. Phys. **105**, 103703 (2009).

[17] M.J. Kendrick, A. Neunzert, M.M. Payne, B. Purushothaman, B.D. Rose, J.E. Anthony, M.M. Haley, and O. Ostroverkhova, J. Phys. Chem. C **116**, 18108 (2012).